

Influence of tensile stress on permeability properties of type 304 stainless steel

K. Kinoshita

Citation: [Journal of Applied Physics](#) **117**, 17B713 (2015); doi: 10.1063/1.4913819

View online: <http://dx.doi.org/10.1063/1.4913819>

View Table of Contents: <http://scitation.aip.org/content/aip/journal/jap/117/17?ver=pdfcov>

Published by the [AIP Publishing](#)

Articles you may be interested in

[Nondestructive evaluation of residual stresses in case hardened steels by magnetic anisotropy measurements](#)

AIP Conf. Proc. **1430**, 1445 (2012); 10.1063/1.4716386

[Physical aging of plastoferites under tensile stress and its effect on microwave properties](#)

J. Appl. Phys. **104**, 064108 (2008); 10.1063/1.2978223

[Dynamic magnetomechanical properties of Terfenol-D/epoxy pseudo 1-3 composites](#)

J. Appl. Phys. **97**, 10M308 (2005); 10.1063/1.1851889

[Dependence of power losses on tensile stress for Fe–Si nonoriented steel up to destruction](#)

J. Appl. Phys. **91**, 7854 (2002); 10.1063/1.1446117

[Experimental study of laser-driven shock waves in stainless steels](#)

J. Appl. Phys. **84**, 5985 (1998); 10.1063/1.368894



Influence of tensile stress on permeability properties of type 304 stainless steel

K. Kinoshita^{a)}

Department of Energy Conversion Science, Graduate School of Energy Science, Kyoto University,
Yoshida-honmachi, Sakyo-ku, Kyoto 606-8501, Japan

(Presented 6 November 2014; received 22 September 2014; accepted 27 October 2014; published online 4 March 2015)

The permeability properties of type SUS304 stainless steel (SUS304 steel) were evaluated under different values of tensile stress using the electromagnetic impedance method. The impedance–magnetic-field curve of SUS304 steel, which corresponds to the permeability–magnetic field-curve, was measured under tensile stresses of 0, 70, and 140 MPa for specimens subjected to prestrains of 5% to 40% to change the martensite fraction. The impedance curves were measured in the length (tensile) direction and the width direction. The results showed that the tensile direction was the magnetic hard axis of the martensite phase in SUS304 steel. The applied stress sensitivity of the permeability in SUS304 steel was affected by the volume fraction, residual stress, stress distribution according to the orientation angle of the martensite phase, and their interactions. © 2015 AIP Publishing LLC. [<http://dx.doi.org/10.1063/1.4913819>]

I. INTRODUCTION

The ferromagnetic martensite phase (m-phase) of austenitic SUS304 steel is induced by plastic deformation. We have previously proposed using this m-phase formed during production and machining as an indicator of deterioration and have investigated the magnetic properties of the phase.^{1,2} The magnetic properties were confirmed to strongly depend on the volume fraction, aspect ratio, and orientation angle of the m-phase, as well as on the internal stress. However, the effect of internal stress on the magnetic properties has only been evaluated before and after annealing,¹ without a detailed investigation. Although it has been previously reported³ that the internal stress has a possible effect on the magnetic properties of the m-phase, a detailed survey has been not conducted. Moreover, it is difficult to accurately induce internal stress in a specimen.

In this study, the permeability properties of SUS304 steel were measured under different tensile stress values using an electromagnetic impedance (EMI) method,^{1,2} and the dependence of the permeability properties of the m-phase on the applied stress was evaluated. The permeability properties were measured along the length and width for specimens subjected to prestrains of 5% to 40% to assess the relationship between the martensite structure and applied stress.

II. THEORY

The shape, distribution mode, and orientation distribution of the m-phase generated in SUS304 steel by plastic deformation are dependent on the mechanical test conditions.^{2,4,5} In the case of plain tensile deformation,² needle-like m-phase particles are orientated at nearly 45° to the load direction at a prestrain of 5%, and the orientated

angle decreases with increasing prestrain. Therefore, because the m-phase stress generated by applied stress changes with the amount of prestrain, it is important to understand the relationship between the internal stress, orientation angle, and permeability of the m-phase. Figure 1 shows a schematic illustration of SUS304 steel when the needle-like m-phase particle is modeled as a single, two-dimensional, ellipsoidal inhomogeneity for simplicity. The x_1 and x_2 axes are along the directions of the specimen's length and width, respectively. The x_1' and x_2' axes are the m-phase particle's long and short axes directions, and θ is the orientation angle between the x_1 and x_1' axes. When tensile stress σ_0 is applied along the x_1 axis, the elastic modulus and Poisson's ratio of the austenite phase (a-phase) and m-phase, as well as the aspect ratio of the m-phase, determine the stress condition in the m-phase.⁶ However, because the mechanical properties of the m-phase have not been measured yet, the same mechanical properties are considered for both the a-phase and m-phase in many cases.⁷ As a result, the stress of the

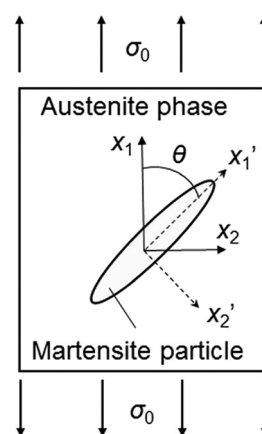


FIG. 1. Schematic of martensite particle model under tensile stress.

^{a)}Electronic mail: kinoshita@energy.kyoto-u.ac.jp.

m-phase in the x_1' - and x_2' -directions is determined by σ_0 and θ , as shown in Eq. (1)⁸

$$\sigma_1' = \sigma_0 \cos^2 \theta, \quad \sigma_2' = \sigma_0 \sin^2 \theta. \quad (1)$$

In this study, because specimens without heat treatment were used, the effect of residual stress generated by the prestrain must be added to Eq. (1). Heat treatment was omitted to investigate the characters of such practical materials because most SUS304 steel, such as the #400 finish, contains the m-phase formed during production and machining and is used without stress relief annealing after processing. When tensile stress was applied along the x_1 -direction, the amounts of plastic strain in the x_1 -direction in the a-phase and m-phase were different because the proof stress of the m-phase was higher than that of the a-phase. The difference in plastic strain thus generated internal tensile stress in the x_1 -direction of the m-phase after unloading.⁹ Without applied stress along the x_2 -direction, the difference in residual strain in the x_2 -direction generated internal compressive stress, which is opposite to the tensile stress along the x_1 -direction. Because elastic stress was applied to the specimens, if the residual stresses in the x_1 - and x_2 -directions are defined as σ_1^r and σ_2^r , respectively, the m-phase stresses in the x_1' - and x_2' -directions can be calculated by superposition, as shown in the following equations:

$$\sigma_1' = (\sigma_0 + \sigma_1^r) \cos^2 \theta + \sigma_2^r \sin^2 \theta, \quad (2)$$

$$\sigma_2' = (\sigma_0 + \sigma_1^r) \sin^2 \theta + \sigma_2^r \cos^2 \theta. \quad (3)$$

Because plastic deformation satisfies the incompressibility condition, the residual strain in the x_2 -direction is half of that in the x_1 -direction. Therefore, as the tensile stress σ_1^r is greater than the compressive stress σ_2^r , σ_1' and σ_2' are components of the tensile stress with the same magnitude at $\theta = 45^\circ$.

We assume that the permeability in an arbitrary direction depends only on the stress in the same direction. The permeabilities in the x_1' - and x_2' -directions are defined as a function of σ_1' , μ_1' (σ_1'), and a function of σ_2' , μ_2' (σ_2'), respectively, and the permeabilities in the x_1 - and x_2 -directions are obtained by performing coordinate transformation. The EMI method measures the impedance as a manifestation of the permeability that is changed by a static magnetic field. When a magnetic field is applied in only one direction, which is the same direction in which the permeability is measured, the permeability along the measurement direction is given as follows:

$$\mu_1 = \mu_1'(\sigma_1') \cos^2 \theta + \mu_2'(\sigma_2') \sin^2 \theta$$

if the magnetic field is in the x_1 -direction, (4)

$$\mu_2 = \mu_1'(\sigma_1') \sin^2 \theta + \mu_2'(\sigma_2') \cos^2 \theta$$

if the magnetic field is in the x_2 -direction. (5)

From Eqs. (4) and (5), it is predicted that μ_1 and μ_2 exhibit similar behavior to σ_0 at $\theta = 45^\circ$.

III. EXPERIMENTAL

The specimens were cold-rolled SUS304 steel plates (2B finish), which had a dumbbell shape with parallel lengths of 146 mm, and a thickness of 3 mm, subjected to prestrains of 5% to 40% to change the martensite fraction. Tensile stress was applied by a tensile testing machine, and the stress values were 70 and 140 MPa, below the proportional limit of 150 MPa. A rectangular coil with dimensions of $6 \times 8 \times 1 \text{ mm}^3$ was used for measuring impedance, and the wire had a diameter of $60 \mu\text{m}$. The winding numbers of the coil for the measurements in the length and width directions were 195 and 197 turns, respectively. The impedance was measured using an LCR meter (lift-off distance = $20 \mu\text{m}$, AC frequency = 3.5 MHz, AC voltage = 0.5 V). The test proceeded as follows. A load was applied to a predefined stress value, which was maintained. After demagnetization, the coil impedance was measured only during periods when the magnetic field was maintained using an electromagnet, and the impedance–magnetic-field relation (impedance curve) was obtained. An exact formula cannot be derived for the permeability, because the impedance curve of ferromagnetism is nonlinear. Therefore, the impedance curve was fitted to the exponential function given by Eq. (6), and deterioration such as fatigue was evaluated using the coefficients

$$\Delta Z = (Z(H) - Z(H_{I=0})) / Z(H_{I=0}) = \alpha \exp(-\beta H) + \delta H + \gamma, \quad (6)$$

where ΔZ is the rate of impedance change, I is an excitation current of the electromagnet, and H is the magnetic field. Although α , β , γ , and δ in Eq. (6) are evaluation parameters, the value of ϕ , calculated using Eq. (7), was used to evaluate the permeability properties in this study.

$$\phi = \left| \int_0^{200} \{ \alpha \exp(-\beta H) + \delta H + \gamma \} dH \right|. \quad (7)$$

The martensite fraction of the specimens was calculated by assigning the value of α obtained in the experiments to the function of α versus m-fraction obtained using results from the literature.³

IV. RESULTS AND DISCUSSION

Figure 2 shows the relationship between ϕ^L , obtained from the ΔZ curve in the length direction, and tensile stress. The superscript L indicates the length direction, and \bullet and \circ represent the result of the two specimens with the same prestrain; the martensite fraction of \bullet is higher than that of \circ . For specimens subjected to prestrains other than 10% and 20%, ϕ^L decreases with increasing tensile stress. Because a decrease in ϕ^L indicates a decrease in the variation of the permeability of the m-phase, the direction of the tensile stress is along the magnetic hard axis of the m-phase. Conversely, when the prestrains are 10% and 20%, ϕ^L does not decrease with increasing tensile stress and change randomly. Table I shows the martensite fraction V_f and $\Delta \phi^L$, which is the average of the difference in ϕ^L obtained under tensile stresses of 0 and 140 MPa for specimens subjected to

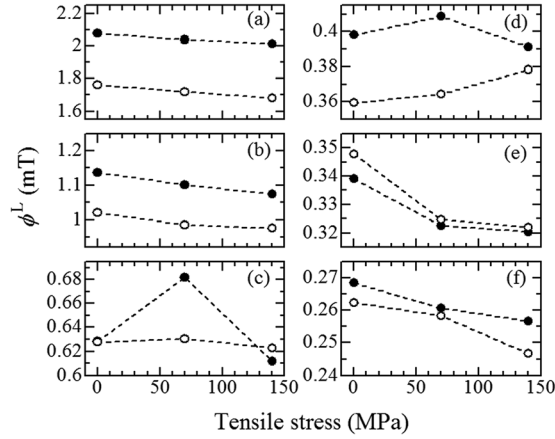


FIG. 2. Relationship between ϕ^L and prestrain under different tensile stresses at a prestrain of (a) 40%, (b) 30%, (c) 20%, (d) 10%, (e) 5%, and (f) 0%.

TABLE I. Martensite fraction V_f and $\Delta\phi^L$ which is the average of the difference in ϕ^L obtained under tensile stresses of 0 and 140 MPa for specimens subjected to the same prestrain.

Prestrain (%)	V_f (%)	$\Delta\phi^L$ (mT)
40	3.8	0.068
30	1.3	0.055
20	0.46	0.010
10	0.19	0.0060
5	0.17	0.022
0	0.14	0.014

the same prestrain. The values of $\Delta\phi^L$ for specimens subjected to prestrains of 10% and 20% are much lower than those of other specimens, which means that their ΔZ curve is almost unchanged by tensile stress. However, more detailed work is necessary to resolve this issue. Because $\Delta\phi^L$ increases with the martensite fraction V_f , a correlation exists between V_f and the stress dependency of the ΔZ curve.

Figure 3 shows the relationship between ϕ^T obtained from the ΔZ curve in the width direction and the tensile stress; the superscript T indicates the width direction. ϕ^T also decreases with increasing tensile stress, except for prestrains of 10% and 20%. Therefore, when the m-phase particles are oriented at nearly 45° to the load direction, the μ_2 in the x_2 -direction shows the same dependence on tensile stress as the μ_1 in the x_1 -direction, as predicted by Eqs. (4) and (5). Figure 4 shows the relationship between both $\Delta\phi^L$ and $\Delta\phi^T$ and the prestrain. $\Delta\phi^L$ increases almost linearly with increasing prestrain, except for prestrains of 10% and 20%. However, $\Delta\phi^T$ of the specimen prestrained at 5% is somewhat lower than that of the specimen prestrained 0%, and the relationship between $\Delta\phi^T$ and prestrains of 0%, 30%, and 40% is not linear. As described in Sec. II, the orientation angle of the m-phase particles to the load direction changes from 45° to 0° with increasing prestrain. Because the martensite fraction in the specimen subjected to a prestrain of 5% is almost unchanged compared with that in the specimen subjected to a prestrain of 0% (Table I), the change in $\Delta\phi^T$ is dependent on θ , σ_1^r , and σ_2^r . Figure 5 shows the relationship between σ_2^r and θ under various values of

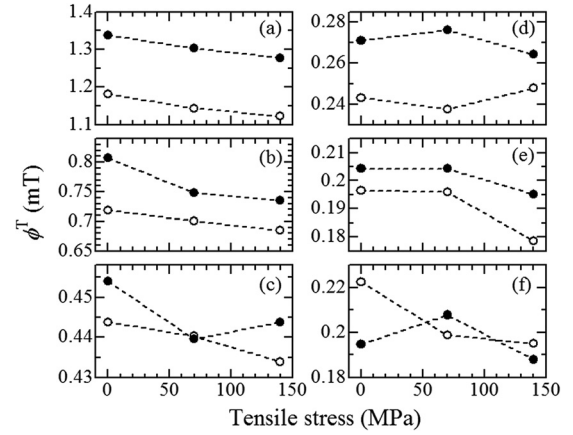


FIG. 3. Relationship between ϕ^T and prestrain under different tensile stresses at a prestrain of (a) 40%, (b) 30%, (c) 20%, (d) 10%, (e) 5%, and (f) 0%.

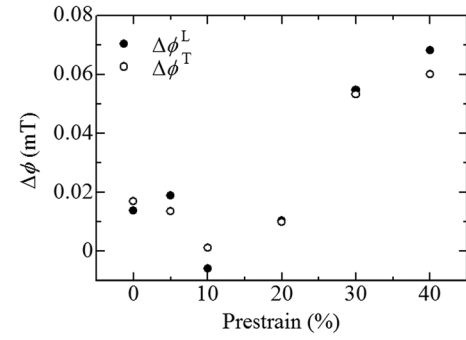


FIG. 4. Relationships between both $\Delta\phi^L$ and $\Delta\phi^T$ and the prestrain.

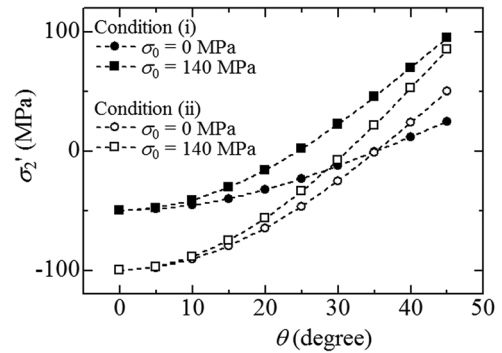


FIG. 5. Relationships between stress in the x_2' -direction and orientation angle under different tensile stresses represented by conditions (i) and (ii).

tensile stress using Eq. (3), when conditions (i) $\sigma_1^r = 100$ MPa, $\sigma_2^r = -50$ MPa, or (ii) $\sigma_1^r = 200$ MPa, $\sigma_2^r = -100$ MPa are assumed. The value of σ_2^r decreases with decreasing θ under all conditions, and σ_2^r decreases more under condition (ii) than under condition (i). The difference between values of σ_2^r corresponding to $\sigma_0 = 0$ and 140 MPa is smaller under condition (ii) than under condition (i). Therefore, because θ at a prestrain of 5% is smaller than that at a prestrain of 0%, and because σ_1^r and σ_2^r at a prestrain of 5% are larger than the corresponding values at a prestrain of 0%, $\Delta\phi^T$ at a prestrain of 5% is somewhat lower than $\Delta\phi^T$ at a prestrain of 0%. Further, because the values of

$\Delta\phi^T$ at prestrains of 30% and 40% are also dependent on the martensite fraction, the non-linearity of $\Delta\phi^T$ cannot be explained by the above scenario alone. However, to explain the large variation in the value $\Delta\phi^T$ at a prestrain of 30%, more experiments are necessary.

V. CONCLUSION

In summary, it is shown that the tensile-stress direction is the magnetic hard axis of the martensite phase in SUS304 stainless steel. However, the tensile stress dependency of the permeability was not observed at specific prestrains (10% and 20%). When the martensite phase particles are oriented at nearly 45° to the load direction, the permeability in the width direction shows the same dependence on tensile stress as the one in the length direction, as predicted theoretically. The sensitivity of the permeability in prestrained SUS 304 stainless steel to applied stress is affected by the volume fraction, residual stress, stress distribution according to the orientation angle in the martensite phase, and their

interactions. When the prestrain is less than 5% and the volume fraction hardly increases, the variation of stress distribution according to the orientation angle in the martensite phase is clear.

ACKNOWLEDGMENTS

This work was supported by Grant-in-Aid for Scientific Research (C) (No. 23560503).

¹K. Kinoshita *et al.*, *Int. J. Appl. Electromagn. Mech.* **39**, 375 (2012).

²K. Kinoshita *et al.*, *Int. J. Appl. Electromagn. Mech.* **45**, 45 (2014).

³K. Mumtaz *et al.*, *J. Mater. Sci.* **39**, 85 (2004).

⁴T. Iwamoto *et al.*, *Int. J. Mech. Sci.* **40**, 173 (1998).

⁵Y. Uematsu *et al.*, *J. Soc. Mater. Sci., Jpn.* **62**, 744 (2013).

⁶T. Mura, *Micromechanics of Defects in Solids*, 2nd revised ed. (Kluwer Academic, Dordrecht, 1987).

⁷N. Tsuchida *et al.*, *J. Jpn. Inst. Met.* **72**, 769 (2008) (in Japanese).

⁸J. M. Gere and S. P. Timoshenko, *Mechanics of Materials*, 4th SI ed. (Stanley Thornes, Delta Place, 1999), p. 477.

⁹A. Takimoto *et al.*, *Trans. JSME* **55**, 1909 (1989) (in Japanese).